Energy-Efficient Base-Station Cooperative Operation with Guaranteed QoS

Feng Han, *Student Member, IEEE,* Zoltan Safar, *Member, IEEE,* and K. J. Ray Liu, *Fellow, IEEE*

***Abstract*—With the explosive deployment of the information and communications technology (ICT) infrastructures, the rising cost of energy and increased environmental awareness has sparked a keen interest in the development and deployment of energy-efficient communication technologies. As a major player in the ICT sector, the energy efficiency of the mobile cellular networks can be significantly improved by switching off some base stations during off-peak periods. In this paper, we propose an energy-efficient BS switching strategy, and use cooperative communication techniques among the base stations to effectively extend network coverage. We incorporate both the path-loss and fading effects in our system model, and derive closed-form expressions for two important quality of service metrics, the call-blocking probability and the channel outage probability. The proposed scheme guarantees the quality of service of the user equipments by identifying the user equipments situated at the worst-case locations. The energy-saving performance is evaluated and compared with the conventional uni-pattern operation. Both analytical and numerical results show that the proposed energy-efficient switching strategy, facilitated by BS cooperation, can provide significant energy-saving potential for the cellular networks with guaranteed quality of service.**

***Index Terms*—Energy efficiency, base station switching, base station cooperation, quality of service.**

I. Introduction

THE Information and Communications Technology (ICT) industry has experienced an explosive growth during the past few decades, and it continues to grow rapidly. Consuming roughly 900 billion KWh per year, the ICT infrastructure is responsible for about 10% of the world's electric energy consumption [1]. Within the ICT sector, the mobile telecommunication industry is one of the major contributors to energy consumption.

In addition to the environmental impact, electric energy consumption is also an important economic issue. Reports show that nearly half of the total operating expenses for a mobile telecommunication operator is the energy cost [2]. Therefore, an energy-efficient cellular network operation is needed more than ever before to reduce both the operational expenses and the carbon footprint of this industry.

In a typical cellular system, base stations (BSs) contribute 60%-80% of the energy consumption of the whole network [3]. Thus, improving the energy-efficiency of the BSs can significantly reduce both the operational cost and carbon footprint. However, the deployment and network operation of BSs have mainly focused on optimizing capacity, coverage, and data rates, instead of energy consumption until recently [3]–[11]. One way to achieve this is to reduce the power consumption of an active BS by, for example, designing more efficient power amplifiers or decreasing the distance between the BS hardware and the antennas. However, these approaches have only a limited impact on the overall power-efficiency of the BS since its energy consumption is dominated by components that simply keep a BS active, which do not depend on the traffic load. As an example, a typical active BS consumes 800-1500 W, while its power amplifier output is only 40-80 W during the high-traffic hours [4]. This means that a BS consumes more than 90% of its peak consumption under the conventional operation even in periods of idle operation. On the other hand, as shown in [5], the sinusoid-like BS traffic profile exhibits large peak-to-peak variations during a typical daily cycle. Therefore, to achieve better energy efficiency, one can take a more efficient operation in which some BSs are turned off in the network in a coordinated manner, and the corresponding traffic load is distributed among the remaining active BSs when the overall network traffic load is low (e.g. during nights, weekends, and holidays).

A. Related Work

Among previous works on energy saving by BS operation management mechanisms, the authors of [6] proposed turning off half of the BSs in a regular pattern and analyzed the call blocking probability and the average number of active calls as functions of the call generation rate. In [3] and [5], the amount of saved energy was characterized for different temporal traffic patterns and switching strategies. A centralized and a decentralized BS switching algorithm in [7] assigned "active" or "sleep" states to BSs and users to "active" BSs based on the transmission rate requirements of the users and the capacity of the BSs. To lower the energy consumption, a hierarchical cellular architecture was proposed in [8], where additional microcells provided increased capacity during peak hours, but these microcells were turned off during periods with low traffic demand, resulting in a more energy-efficient cellular system. Algorithms for the deployment and operation of such a hierarchical network were proposed in [9] based on the notion of area spectral efficiency. In [12], the cellular network greening effect was studied under four combinations of spatial-temporal power sharing policies, facilitated by short-term (per each time slot) BS transmit power control with global BS total power budget. The authors of [11] looked at the energy-saving potential and investigated the impacts of traffic

Manuscript received September 30, 2012; revised January 10 and April 19, 2013. The editor coordinating the review of this paper and approving it for publication was E. Au.

The authors are with the Department of Electrical and Computer Engineering, University of Maryland, College Park, MD, 20742 USA (e-mail: {hanf, zsafar, kjrliu}@umd.edu).

Digital Object Identifier 10.1109/TCOMM.2013.061913.120743

intensity and BS density to the energy saving performance within the context of the LTE-Advanced cellular standard with coordinated multi-point (CoMP) transmission and wireless relaying. The authors of [10] considered the scenario where two operators share the same BS during low traffic periods and analyzed the achievable energy savings.

After switching off some BSs, the service areas of the remaining active BSs increase, reducing the signal to noise ratio (SNR) at the receiver side considerably due to increased distances between the active BSs and the user equipments (UEs). Most previous works did not consider the quality of service (QoS) degradation due to this path-loss effect [13]–[15]. In this work, we take into account both path-loss and fading of wireless channels, and guarantee the QoS of UEs while achieving energy saving.

The last decade witnessed a lot of progress in cooperative communications [16], which can be used to effectively extend the network coverage with reduced transmit power [17]. For typical outdoor wireless environments, the path loss exponent can be between 3 and 4. This means that when the distance doubles, the required transmit power will increase at least eight-fold to maintain the same received SNR without BS cooperation. Such a penalty of increased transmit power may considerably diminish the energy saving gained by turning off BSs, which makes the BS cooperation an enabling technique for the energy-efficient BS-switching operations.

B. Our Approach

In this paper, we propose an energy-efficient BS switching strategy for cellular systems and use BS cooperation to effectively extend the network service to the areas of the switched-off BSs. Specifically, based on the standard hexagonal cell model [18], [19][1], we consider four progressive BS switch-off patterns and dynamically switch among them according to the traffic load to maximize energy saving. We study the QoS of the resulting cellular system in terms of the call-blocking probability and the channel outage probability, from both the network-layer and the physical-layer perspectives, respectively. We derive and analyze the closed-form expressions for the QoS metrics based on the hexagonal cell model. As will be shown in this paper, the call-blocking probabilities associated with different switch-off patterns characterize a feasible set of patterns to choose from so that the minimum requirement (on the call-blocking probability for any UE) is satisfied for the given offered load. We guarantee the channel outage probability by identifying the UEs situated at the worst-case locations and use BS cooperation to ensure their minimum QoS requirements. We evaluate the achievable energy saving performance of the proposed scheme and compare them with the conventional network operation.

The rest of this paper is organized as follows: In Section II, we describe the system model and QoS metrics used in this paper. In Section III, we introduce four BS switch-off patterns and calculate their associated call-blocking probabilities. In Section IV, we investigate the channel outage probability of an established channel link, taking into account the impact of the offered load to the availability of active BSs in the cooperation. We model and calculate the energy consumption of the BS under the proposed BS switching patterns in Section V. Section VI presents the numerical results of the system performances and demonstrate the energy-saving potential of this proposed scheme. Finally, conclusions are drawn in Section VII.

[1]Although regular hexagonal cells hardly exist in real life, the practical deployment of macrocell BSs is always well planned and never random. More importantly, the regularity of such a widely used hexagon model facilitates clear and insightful analysis in the literature, as well as in this paper. The intention of this paper is not to directly solve the detailed real-life problems; rather, it strives to show that the ideas proposed in this work can lead to significant energy-saving potential to cellular networks.

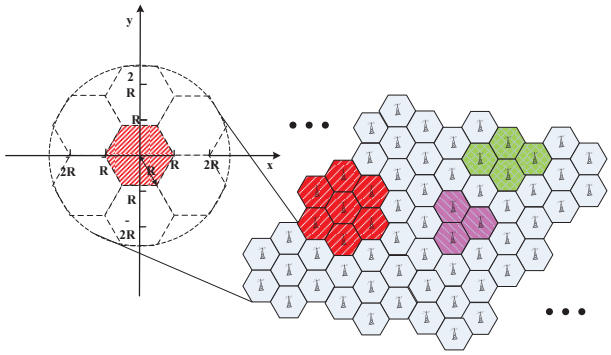

Fig. 1. A local dense-deployment area covered by hexagonal cells.

II. System Model

A. Network Model

We consider a standard cellular network model consisting of hexagonal cells with radius R, and each cell is equipped with a multi-antenna BS located in the center of the cell, as shown in Fig. 1. In such a network, the fractional frequency reuse is assumed with the neighboring cells allocated with different bandwidths. The BSs are inter-connected with backhaul links, through which communications are assumed to be low-cost, reliable and high-speed. Each BS has M antennas, and the UEs served by this network have one single antenna.

We assume that in each cell call requests arrive following a Poisson process with an arrival rate $\lambda(t)$ at time t, and the call holding time has an expected value $1/\mu$. Consequently, each cell provides an *offered load* of $E(t) = \lambda(t)/\mu$ (Erlang) to the cellular infrastructure. For simplicity, we further assume that the offered loads from different cells are independent and identically distributed (i.i.d.).

We consider that each BS has a limited capacity to serve a maximum number of active concurrent UEs due to its limited hardware and software resources [20][2]. This number is denoted by C in this paper. Note that such a limitation is inherent at the BS and is not necessarily related to the scarcity of channel resources. It means that even when there are ample amount of available channel resources like the case of low traffic hours, an individual BS has to reject a new UE's request if the number of concurrent UEs at this BS will otherwise exceed C.

[2]When a UE is served by multiple BSs through cooperation, this UE accounts for an active UE at each of the BSs that participate this cooperation.

B. Channel model and Cooperative Coverage Extension

Let $h_k^{(m)}$ denote the fading channel coefficient between a UE and the m-th antenna of the k-th BS. $h_k^{(m)}$ is modeled as circularly symmetric complex Gaussian random variables with zero mean and variance

$$\sigma_k^2 = \frac{G}{d_k^\alpha}, \tag{1}$$

where d_k is the distance between the k-th BS and the UE, α is the path loss exponent [15], [21], and G is a normalizing gain factor. Assume that different $h_k^{(m)}$ are uncorrelated, and that the channel state information is available at the BS side.

To efficiently extend coverage to the service areas of the switched-off BSs and compensate the SNR loss due to increased BS-UE distances, the nearby active BSs will use cooperative communications. We limit the set of cooperating BSs to the six direct neighboring BSs of the switched-off cells.

When a BS is switched off, it releases its channel resources to its neighboring active BSs. Then the neighboring active BSs use the channel resources obtained from the switched-off BS to cooperatively serve (using cooperative beamforming) the UEs inside the switched-off cell (referred to as, the *moon cell* in the sequel). In the cells having an active BS (referred to as, the *sun cell*), the UEs are served by the single active BS the same way as in the conventional operation without BS cooperation. Since the traffic load during these off-peak-traffic hours is lower than during peak hours, we assume that during the energy-efficient operations, the available channel resources can accommodate the reduced overall traffic load by adopting certain interference management scheme [22]. Similar to [7] [11], it is also assumed that the use of cooperative beamforming [23] will not cause a noticeably higher inter-cell interference level compared to the conventional operation. Such an assumption simplifies the analytical derivations, and at the same time can be justified as follows:

- Compared with the conventional cell-breathing scheme (i.e. by simply increasing BS's transmit power) [3], the cooperative beamforming can steer the transmitted signals towards only the intended location where the signals are summed constructively, which effectively reduces the required total transmit power; on the other hand, thanks to the spatial selectivity of cooperative beamforming, the interference signals will be summed destructively at the victim cells, whose power can be expected no much higher than the conventional operation.
- Second, when the fractional frequency reuse is used in this network, two cells that use the same frequency band are separated by a distance. Considering the propagation loss in cellular systems, the interference power is further attenuated when it arrives at the victim cell.
- Third, although it is true that some neighboring cells can be closer to the victim cell, in the BS cooperation, each of the cooperating BSs only needs to transmit just a fraction of the total transmit power, which further eases its interference power to its neighboring cells.

For the UEs inside a moon cell, the cooperative coverage extension schemes for both downlink and uplink are specified as follows:

1) Downlink: Since the channel state is known at the BS side, the optimum cooperative transmission scheme is *cooperative transmit beamforming* which maximizes the received SNR at the UE [23]. The resulting SNR at the UE (receiver) is given by:

$$SNR = \sum_{k=1,m=1}^{K,M} \frac{|h_k^{(m)}|^2 P_{\mathrm{BS}}}{N_{\mathrm{UE}}} = \frac{P_{\mathrm{BS}}}{N_{\mathrm{UE}}} \sum_{k=1,m=1}^{K,M} |h_k^{(m)}|^2, \tag{2}$$

where P_{BS} is the total transmit power of all the cooperating BSs[3], N_{UE} is the noise power at the UE, and K is the number of cooperating BSs. Note that in (2), we ignore the interference from other cells for analytical simplicity, given the assumption that the use of cooperative beamforming will not cause a noticeably higher inter-cell interference compared to the conventional operation.

2) Uplink: For uplink, given that the channel state information is available at the BS side, *Maximal Ratio Combining* (MRC) [21], [24] can be achieved by cooperative receive beamforming among cooperating BSs. The resulting SNR at the BS (receiver) side is

$$SNR = \sum_{k=1,m=1}^{K,M} \frac{P_{\mathrm{UE}}|h_k^{(m)}|^2}{N_k^{(m)}}. \tag{3}$$

where P_{UE} is the transmit power of the UE, and $N_k^{(m)}$ is the noise power received at the m-th antenna of the k-th BS. For simplicity, we further assume that $N_k^{(m)}$ are identical for all k and m, i.e. $N_k^{(m)} = N_{\mathrm{BS}}$, then

$$SNR = \frac{P_{\mathrm{UE}}}{N_{\mathrm{BS}}} \sum_{k=1,m=1}^{K,M} |h_k^{(m)}|^2. \tag{4}$$

Due to the same structure of uplink and downlink shown in (2) and (4), we could use a unified expression

$$SNR = \sum_{k=1,m=1}^{K,M} \frac{P}{N}|h_k^{(m)}|^2. \tag{5}$$

where P and N denote the transmit power and the receiver noise variance, respectively.

C. Quality of Service Metrics

In this paper, we propose an energy-efficient BS switching strategy according to the varying offered traffic load. However, the energy-saving purpose makes sense only when the QoS of a UE is guaranteed to be above a certain required level. In this paper, we consider and derive the closed-form expressions for two QoS metrics:

- *Call-Blocking Probability*: how likely a UE's request is rejected by the infrastructure due to limited resources.
- *Channel-Outage Probability*: given that a UE's request is not rejected (therefore, a link is established between

[3]In order to achieve the SNR level shown in (2), the m-th antenna of the k-th BS transmits with a fraction of the total transmit power $\left(|h_k^{(m)}|^2\right) \Big/ \left(\sum_{k=1,m=1}^{K,M} |h_k^{(m)}|^2\right)$. Therefore, we assume that each individual power constraint (limited by the power amplifier) on each antenna and/or BS can be satisfied, and mainly focus on the total transmit power consumption.

this UE and available BS(s)), for a certain given SNR threshold γ_0, how likely the instantaneous received SNR level of the established link is lower than γ_0 due to channel fading.

During the off-peak-traffic hours, some BSs are switched off to save energy. The traffic of the service areas of the switched-off BSs is distributed to the remaining active BSs, which leads to a higher aggregated traffic load for each of the remaining active BSs. For a given offered load per cell, the more BSs are turned off, the more UEs' requests need to be addressed by each active BS. Therefore, the QoS requirement on the call-blocking probability in essence serves as a constraint for the BS switch-off pattern selection. Given that a UE's request has been accepted by the infrastructure, we can then use channel outage probability to measure the quality of the established channel link. In this paper, we guarantee QoS by targeting at the UEs situated at the worst-case locations in the network.

III. BS Switching Patterns and the Call-Blocking Probabilities

In this section, we introduce four BS switching patterns that progressively turn off more BSs according to the offered traffic load. Then, we calculate the call-blocking probability associated with each pattern.

A. BS Switch-off Patterns

As the offered traffic load goes low, some of the BSs are switched off, resulting in a more energy-efficient network operation, and the corresponding traffic load is distributed among the remaining active BSs. In determining which BSs to switch off in a large-scale network according to varying offered load, the optimal solution involves integer programming, which is proven to be NP-hard [25], [26]. Some previously proposed suboptimal algorithms [7], [9] did not consider the possibility of BS cooperation in their objective functions. Moreover, even though an optimal solution is available for any given offered load, the operational complexity of constantly switching BSs on and off according to the continuously varying offered load is not affordable for practical use. Therefore, we propose to use a set of BS switching patterns which consist of scalable building blocks to cover the cellular network. Specifically, we consider four switch-off patterns in the context of BS cooperation as shown in Fig. 2.

In Fig. 2, the diagram of the switch-off pattern I visualizes a basic switching pattern and the resulting cooperation topology when one BS is switched off in a basic building block of seven BSs. In this pattern, each moon cell is served by up to six[4] neighboring BSs through cooperative communications. We will refer to this case as *pattern I* for short in the sequel. Similarly, three more switch-off patterns II, III, and IV are also presented in Fig. 2, corresponding to switching off one BS out of three BSs, switching off two BSs out of four BSs, and switching off three BSs out of four BSs, respectively.

Among a very large number of possible switching patterns, the four switch-off patterns are heuristically chosen as the formations of small regular building blocks, provided that the density of the users is roughly uniform across the cellular network. The regularity brought by these patterns offers great scalability for a large-scale deployment. Furthermore, after being deployed across the network, each of the four patterns results in the same cooperation topology for any moon cell (regardless its location) under that pattern, as shown in Fig. 2. Such system-wide homogeneity simplifies the analysis complexity and leads to a unified system analysis for each moon cell. As one can see from Fig. 2, the four switch-off patterns from I to IV turn off more BSs in a progressive manner to achieve the energy-saving goal with guaranteed QoS. Defining β to be the ratio of the number of switched-off BSs to the total number of BSs for the four switch-off patterns I, II, III, and IV, we obtain $\beta_{\mathtt{I}} = 1/7 = 14.3\%$, $\beta_{\mathtt{II}} = 1/3 = 33.3\%$, $\beta_{\mathtt{III}} = 2/4 = 50.0\%$, and $\beta_{\mathtt{IV}} = 3/4 = 75.0\%$. The conventional operation adopts an *"all-on" pattern*, in which all BSs are active with $\beta_{\mathtt{all\text{-}on}} = 0$.

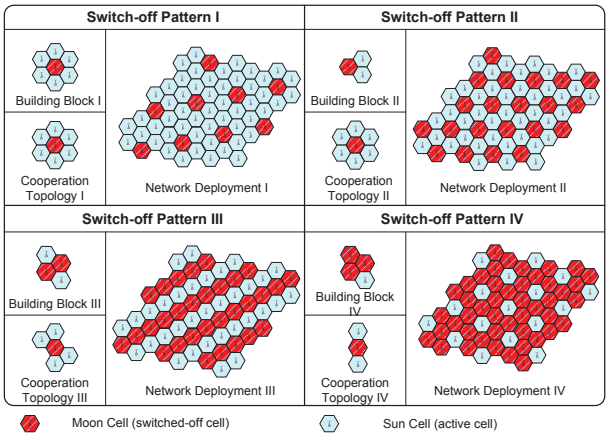

Fig. 2. Scalable switch-off patterns.

Since the traffic loads originating from the moon cells are distributed to active BSs, we calculate the equivalent aggregated traffic load for each active BS in different patterns. Taking switch-off pattern II shown in Fig. 2 for example, each active cell is surrounded by three moon cells that are to be served through cooperating with other active BSs. Unless this active BS is fully occupied, a call attempt from any of these surrounding moon cells will become one additional concurrent UE at this active BS. Therefore, for switch-off pattern II, the aggregated traffic load for each active BS is the sum of the load of its own cell and the loads of all the surrounding moon cells, i.e. $E_{\Sigma,\mathtt{II}}(t) = \frac{(3+1)\lambda(t)}{\mu} = 4E(t)$. Similarly, $E_{\Sigma,\mathtt{I}}(t) = 2E(t)$, $E_{\Sigma,\mathtt{III}}(t) = 5E(t)$, and $E_{\Sigma,\mathtt{IV}}(t) = 7E(t)$. For the conventional operation, $E_{\mathtt{all\text{-}on}}(t) = E(t)$.

Since each active BS only has limited capacity for supporting concurrent UEs, when a UE's request arrives, some BSs may be too busy to help. This gives rise to a set of *cooperating modes* in which some BSs are absent from the basic cooperation topologies shown in Fig. 2 due to limited resources.

The complete set of distinguishable cooperating modes (up to rotations and mirroring) is presented in Fig. 3. Note that different cooperating modes will appear with different relative frequencies depending on the current offered load and the switch-off pattern.

[4]When one or more of the six neighboring active BSs are fully occupied due to the limited capacity C, they cannot help the UE by participating the cooperation.

B. Call-Blocking Probability

In this part, we calculate the call-blocking probability of the UEs in the network under each proposed pattern. We first define two types of call-blocking events for the sun cell and the moon cell, respectively.

Definition 1. (Call Blocking for the Sun Cell) *For any given combination of the single-cell offered load E and switch-off pattern $w \in \{I, II, III, IV\}$, the call-blocking event for the UE in the sun cell occurs when* all the C available resources (for concurrent UEs) of the single BS of this sun cell are fully occupied at the time when the UE's request arrives.

Definition 2. (Call Blocking for the Moon Cell) *For any given combination of the single-cell offered load E and switch-off pattern $w \in \{I, II, III, IV\}$, the call-blocking event for the UE in the moon cell occurs when* all the neighboring BSs that remain active are fully occupied at the time when the UE's request arrives.

Since it is assumed that the traffic arrival process is a Poisson process, we use the Erlang-B formula [27] to calculate the blocking probability for each individual active BS, and then investigate the two types of call blocking probabilities. According to the Erlang-B formula, for a queuing system with C servers but no buffer spaces for incoming service requests to wait, if the service arrival process is a Poisson process that offers a traffic load E, the blocking probability of such a queuing system is given by

$$B(E,C) \triangleq \frac{\frac{E^C}{C!}}{\sum_{i=0}^{C} \frac{E^i}{i!}}, \tag{6}$$

which corresponds to the conventional all-on pattern without BS cooperation.

Applying the Erlang-B formula to Definition 1, the call blocking probability for the sun cell can be calculated as follows:

$$P_{\mathtt{CB,sun}}(E,w) = B\left(E_{\Sigma,w}(E), C\right) = \frac{\frac{E_{\Sigma,w}^C}{C!}}{\sum_{i=0}^{C} \frac{E_{\Sigma,w}^i}{i!}}, \tag{7}$$

where E is the single-cell offered load, $w \in \{I, II, III, IV\}$ represents the switch-off pattern, and $E_{\Sigma,w}(E)$ is the aggregated offered load for the active BS of the sun cell under switch-off pattern w.

From Definition 2, the call-blocking probability of the UE in a moon cell can be written as

$$\begin{aligned} P_{\mathtt{CB,moon}}(E,w) &= Pr\big[\bigcap_{k=1}^{K} \{\text{the } k^{th} \text{ BS is fully occupied}\}\big] \\ &\leqslant Pr\left[\{\text{the } k^{th} \text{ BS is fully occupied}\}\right], \forall k \\ &= P_{\mathtt{CB,sun}}(E,w), \end{aligned} \tag{8}$$

where K is the total number of the neighboring active BSs for this moon cell.

From (8), one can see that the call-blocking probability for the moon cell is always upper-bounded by the one for the sun cell. This is due to the multi-BS diversity brought by the cooperation among multiple neighboring active BSs for the moon cell. For this reason, in order to guarantee the QoS of UEs in both sun cells and moon cells, we need to ensure that $\max\{P_{\mathtt{CB,moon}}(E,w), P_{\mathtt{CB,sun}}(E,w)\} = P_{\mathtt{CB,sun}}(E,w)$ is below a certain threshold, by carefully choosing the switching patterns according to the offered load.

IV. Channel Outage Probability

In this section, we focus on the channel outage probability as a physical layer QoS metric given that a channel link has been established between a UE and the BS(s). If a UE's call-attempt is accepted by the available BSs, a link will be established for this UE. Given the condition that a UE's request is not blocked, the channel outage probability measures the quality of the established link. Specifically, we are looking at a conditional probability that is defined as follows:

Definition 3. *(*channel outage probability*) Conditioned on that a UE's request is not blocked, the channel outage probability for this UE is the conditional probability that the instantaneous SNR for the link established between this UE and BS(s) is lower than a certain threshold γ_0.*

It is worth noting that the channel outage probability defined in this paper is discussed based on the condition that BS(s) can accommodate the UE's request and establish a link for this UE. Therefore, a so defined channel outage probability, as a conditional probability, focus on the quality of the physical channel established between the BSs and the UE.

To guarantee the QoS for all UEs in energy-efficient operations, a spatially averaged QoS metric is not sufficient. Since a UE can be anywhere within the cell, we will focus on the channel outage probability of the UE situated at the worst transmission/reception location within the cell for each cooperating mode shown in Fig. 3. We start with the simple case of the sun cell and the regular cell under the conventional operation, and then investigate the more complicated cases of the moon cell in the following part of this section.

For the sun cell (or equivalently, the regular cell under the conventional operation), the UE is served by just one BS located in the center of the cell. Therefore, the distance between its worst-case location and the BS is the radius of the cell R. The corresponding SNR expression is a special case of (5) with $K = 1$:

$$SNR = \frac{P}{N} \sum_{m=1}^{M} |h_0^{(m)}|^2 = \frac{P}{N} \frac{\sigma_0^2}{2} \sum_{m=1}^{M} \frac{2}{\sigma_0^2} |h_0^{(m)}|^2, \tag{9}$$

where N is the noise power, P is the total transmit power of BS (downlink) or UE (uplink), and $h_0^{(m)}$ is the channel gain between the UE and the m-th antenna of the BS with variance $\sigma_0^2 = \frac{G}{R^\alpha}$.

For ease of simple notation, let $V \triangleq \sum_{m=1}^{M} \frac{2}{\sigma_0^2} |h_0^{(m)}|^2$, which is a central chi-square random variable with $2M$ degrees of freedom. Thus, the channel outage probability for the UE in the sun cell (or equivalently, the UE under the conventional

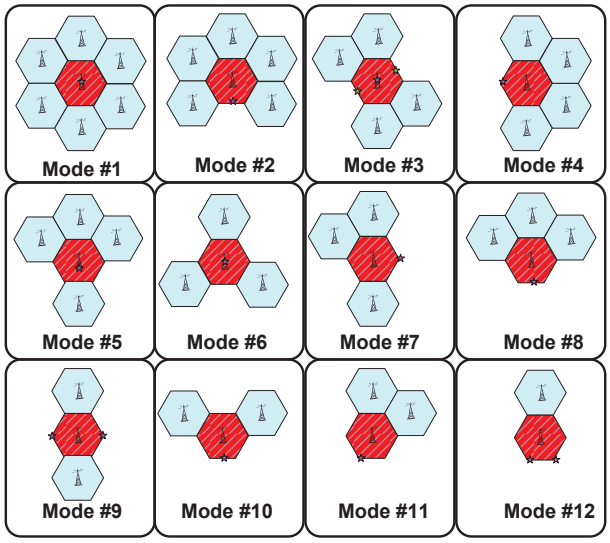

Fig. 3. The complete set of distinguishable cooperating modes.

operation) can be obtained as

$$P_{\text{out}}(sun) = Pr\left[V \leqslant \frac{2\gamma_0 N}{P\sigma_0^2}\right] = \frac{\gamma\left(M, \frac{\gamma_0 N R^\alpha}{PG}\right)}{(M-1)!}, \quad (10)$$

where $\gamma(s,x) = \int_0^x t^{s-1}e^{-t}dt$ is the lower incomplete Gamma function.

For the moon cell, we first identify the worst-case locations for each cooperating modes shown in Fig. 3. Based on that, the channel outage probability of the UE at the worst-case locations is derived for each mode. Finally, we combine the individual channel outage probability of every cooperating mode using the relative frequencies of these cooperating modes that we obtained from computer simulation.

A. Worst-Case Location

To guarantee the channel outage probability of the UEs in the moon cells, the first step is to determine the worst-case location within the moon cell, given the number and locations of the available BSs under each cooperating mode. Fitting their geological locations into a two-dimensional coordinate system as shown in Fig. 1, the BS and UE locations are each assigned a pair of coordinates. Specifically, we assign coordinates to the cooperating BSs and the UE according to

$$BS_1 = (x_1, y_1), \cdots, BS_K = (x_K, y_K);\ UE = (x, y).$$

Then, the distance between the UE and BS_k can be written as

$$d_k = \left[(x-x_k)^2 + (y-y_k)^2\right]^{\frac{1}{2}}. \quad (11)$$

Given the cooperative coverage extension scheme introduced in Section II, the resulting SNR is proportional to the sum $\sum_{k=1,m=1}^{K,M} |h_k^{(m)}|^2$. To determine the worst-case location, we will only need to take into account the effect of path loss by averaging out the fading component:

$$E\left[\sum_{k=1,m=1}^{K,M} |h_k^{(m)}|^2\right] = M\sum_{k=1}^{K}\frac{G}{d_k^\alpha}, \quad (12)$$

TABLE I
SOLUTIONS FOR THE WORST-CASE LOCATION(S) (x^*, y^*)

	♯1	♯2	♯3	♯4	♯5	♯6
$\alpha=3$	$(0,0)$	$\left(0, -\frac{\sqrt{3}R}{2}\right)$	$\pm\left(\frac{\sqrt{3}R}{4}, \frac{3R}{4}\right)$	$(-R, 0)$	$(0, -0.1872R)$	$(0,0)$
$\alpha=4$	$(0,0)$	$\left(0, -\frac{\sqrt{3}R}{2}\right)$	$(0,0)$	$(-R, 0)$	$(0, -0.1478R)$	$(0,0)$
	♯7	♯8	♯9	♯10	♯11	♯12
$\alpha=3$	$(R, 0)$	$\left(0, -\frac{\sqrt{3}R}{2}\right)$	$(\pm R, 0)$	$\left(0, -\frac{\sqrt{3}R}{2}\right)$	$\left(-\frac{R}{2}, -\frac{\sqrt{3}R}{2}\right)$	$\left(\pm\frac{R}{2}, -\frac{\sqrt{3}R}{2}\right)$
$\alpha=4$	$(R, 0)$	$\left(0, -\frac{\sqrt{3}R}{2}\right)$	$(\pm R, 0)$	$\left(0, -\frac{\sqrt{3}R}{2}\right)$	$\left(-\frac{R}{2}, -\frac{\sqrt{3}R}{2}\right)$	$\left(\pm\frac{R}{2}, -\frac{\sqrt{3}R}{2}\right)$

where K is the number of cooperating BSs and M is the number of antennas at each BS.

Consequently, determining the worst-case location within the switched-off hexagonal area is equivalent to solving the following constrained minimization problem:

$$\min_{x,y} \quad f(x,y) = \sum_{k=1}^{K}\frac{1}{\left[(x-x_k)^2 + (y-y_k)^2\right]^{\frac{\alpha}{2}}} \quad (13)$$

$$\text{s. t.} \begin{cases} -\sqrt{3}R \leqslant \sqrt{3}x + y \leqslant \sqrt{3}R; \\ -\sqrt{3}R \leqslant \sqrt{3}x - y \leqslant \sqrt{3}R; \\ -\frac{\sqrt{3}}{2}R \leqslant y \leqslant \frac{\sqrt{3}}{2}R. \end{cases} \quad (14)$$

Since both the objective function and the constrains are continuously differentiable, the Karush-Kuhn-Tucker (KKT) [28] conditions specify the necessary conditions for the solution (x^*, y^*) as follows:

- **Stationarity Condition**

$$\nabla f(x^*,y^*) + (\mu_1-\mu_2)\begin{bmatrix}\sqrt{3}\\1\end{bmatrix} + (\mu_3-\mu_4)\begin{bmatrix}\sqrt{3}\\-1\end{bmatrix} + (\mu_5-\mu_6)\begin{bmatrix}0\\1\end{bmatrix} = 0, \quad (15)$$

where

$$\nabla f(x,y) = \begin{bmatrix}\frac{\partial}{\partial x}f(x,y)\\ \frac{\partial}{\partial y}f(x,y)\end{bmatrix} = \begin{bmatrix}-\alpha\sum_{k=1}^{K}\frac{x-x_k}{\left[(x-x_k)^2+(y-y_k)^2\right]^{\frac{\alpha}{2}+1}}\\ -\alpha\sum_{k=1}^{K}\frac{y-y_k}{\left[(x-x_k)^2+(y-y_k)^2\right]^{\frac{\alpha}{2}+1}}\end{bmatrix}. \quad (16)$$

- **Dual Feasibility Condition**

$$\mu_i \geqslant 0, \quad \text{for all } i = 1, \ldots, 6; \quad (17)$$

- **Primal Feasibility Condition**

$$\begin{cases} -\sqrt{3}R \leqslant \sqrt{3}x^* + y^* \leqslant \sqrt{3}R \\ -\sqrt{3}R \leqslant \sqrt{3}x^* - y^* \leqslant \sqrt{3}R \\ -\frac{\sqrt{3}}{2}R \leqslant y^* \leqslant \frac{\sqrt{3}}{2}R \end{cases} \quad (18)$$

- **Complementary Slackness Condition**

$$\begin{cases} \mu_1\left(\sqrt{3}x^* + y^* - \sqrt{3}R\right) = 0; & \mu_2\left(\sqrt{3}x^* + y^* + \sqrt{3}R\right) = 0; \\ \mu_3\left(\sqrt{3}x^* - y^* - \sqrt{3}R\right) = 0; & \mu_4\left(\sqrt{3}x^* - y^* + \sqrt{3}R\right) = 0; \\ \mu_5\left(y^* - \frac{\sqrt{3}}{2}R\right) = 0; & \mu_6\left(y^* + \frac{\sqrt{3}}{2}R\right) = 0; \end{cases} \quad (19)$$

Leveraging the geological symmetry in each cooperating mode shown in Fig. 3, the worst case location of a UE in the moon cell can be found without much effort from the KKT conditions. Specifically, we have the solution for the worst-case location(s) of each cooperating mode with $\alpha = 3$ (low path loss) and $\alpha = 4$ (high path loss) shown in Table I.

TABLE II
OUTAGE PROBABILITIES OF SYMMETRIC BS ARRANGEMENTS

	K	d	σ^2	P_{out}
♯1	6	$\sqrt{3}R$	$\frac{G}{(\sqrt{3}R)^{\alpha}}$	$\frac{\gamma\left(6M, \frac{\gamma_0 N(\sqrt{3}R)^{\alpha}}{PG}\right)}{(6M-1)!}$
♯3($\alpha=4$)	4	$\sqrt{3}R$	$\frac{G}{(\sqrt{3}R)^{\alpha}}$	$\frac{\gamma\left(4M, \frac{9\gamma_0 N R^{\alpha}}{PG}\right)}{(4M-1)!}$
♯6	3	$\sqrt{3}R$	$\frac{G}{(\sqrt{3}R)^{\alpha}}$	$\frac{\gamma\left(3M, \frac{\gamma_0 N(\sqrt{3}R)^{\alpha}}{PG}\right)}{(3M-1)!}$
♯9	2	$2R$	$\frac{G}{(2R)^{\alpha}}$	$\frac{\gamma\left(2M, \frac{\gamma_0 N(2R)^{\alpha}}{PG}\right)}{(2M-1)!}$
♯10	2	$\frac{\sqrt{21}}{2}R$	$\frac{G}{\left(\frac{\sqrt{21}}{2}R\right)^{\alpha}}$	$\frac{\gamma\left(2M, \frac{\gamma_0 N\left(\frac{\sqrt{21}}{2}R\right)^{\alpha}}{PG}\right)}{(2M-1)!}$
♯11	2	$\sqrt{7}R$	$\frac{G}{(\sqrt{7}R)^{\alpha}}$	$\frac{\gamma\left(2M, \frac{\gamma_0 N(\sqrt{7}R)^{\alpha}}{PG}\right)}{(2M-1)!}$

B. Individual Channel Outage Probability of Each Cooperating Mode

In this part, we analyze the channel outage probability of the UEs situated at the worst-case locations within the switched-off (moon) cell. According to Table I, we divide all the cooperating modes into two categories: the symmetric BS arrangements and the asymmetric BS arrangements. The symmetric arrangements include the cooperating modes $\{\sharp1, \sharp3(\alpha=4), \sharp6, \sharp9, \sharp10, \sharp11\}$, in each of which the neighboring active BSs are equally far away from the worst UE location(s); The asymmetric arrangements include the modes $\{\sharp2, \sharp3(\alpha=3), \sharp4, \sharp5, \sharp7, \sharp8, \sharp12\}$, in which the neighboring active BSs are of different distances from the worst location(s).

1) Symmetric BS Arrangements: For the symmetric cases in Fig. 3, such a symmetric geometry leads to identical channel gain variances $\sigma_k^2 = \frac{G}{d_k^{\alpha}} = \frac{G}{d^{\alpha}}$, for $k = 1, \cdots, K$. Therefore, (5) can be written as

$$SNR = \frac{P}{N}\frac{\sigma_k^2}{2}\sum_{k=1,m=1}^{K,M}\frac{2}{\sigma_k^2}|h_k^{(m)}|^2. \tag{20}$$

Since $W \triangleq \sum_{k=1,m=1}^{K,M}\frac{2}{\sigma_k^2}|h_k^{(m)}|^2$ is a central chi-square random variable with $2MK$ degrees of freedom, the probability $Pr[W \leqslant w]$ (i.e. the CDF of W) is given by

$$Pr[W \leqslant w] = \frac{\gamma(MK, \frac{w}{2})}{(MK-1)!}. \tag{21}$$

Accordingly, the outage probability can be written as

$$P_{\text{out}} = Pr[SNR \leqslant \gamma_0] = \frac{\gamma\left(MK, \frac{\gamma_0 N d^{\alpha}}{PG}\right)}{(MK-1)!}. \tag{22}$$

Applying (22) to $\{\sharp1, \sharp3(\alpha=4), \sharp6, \sharp9, \sharp10, \sharp11\}$, we obtain their channel outage probabilities in Table II.

2) Asymmetric BS Arrangements: For the asymmetric cases shown in Fig. 3, the distances between the worst-case UE location and the cooperating BSs are different. The resulting SNR as shown in (5) can be considered as a linear combination of multiple chi-square random variables. Unfortunately, even for the two-variable case, the exact expression for the SNR distribution is too complicated for practical applications. Thus, we use an approximation developed in [29], whose accuracy has been proven to be very well satisfying in many practical applications [29]–[31].

In doing so, the distribution of the SNR is approximated by that of another random variable $Z = \delta\Psi$, where δ is a scaling factor and Ψ is a central chi-square random variable with s degrees of freedom, such that the expected value and variance of the SNR are equal to those of Z. Specifically,

$$\begin{cases} E[SNR] = \delta E[\Psi] = \delta s \\ Var[SNR] = \delta^2 Var[\Psi] = 2\delta^2 s \end{cases} \tag{23}$$

To show how to apply this approximation to the asymmetric BS arrangements, without loss of generality, we take the cooperating mode ♯7 for example. All the other modes of the asymmetric BS arrangements can be approximated similarly.

For the cooperating mode ♯7, the distances between the worst-case UE location and the three cooperating BSs are $d_1 = \sqrt{7}R$, $d_2 = 2R$, and $d_3 = 2R$, respectively. Then, we can rewrite (5) as

$$SNR = \frac{\sigma_1^2 P}{2N}\sum_{m=1}^{M}\frac{2}{\sigma_1^2}|h_1^{(m)}|^2 + \frac{\sigma_2^2 P}{2N}\sum_{k=2,m=1}^{K=3,M}\frac{2}{\sigma_k^2}|h_k^{(m)}|^2, \tag{24}$$

where $\sigma_1^2 = \frac{G}{(\sqrt{7}R)^{\alpha}}$, and $\sigma_2^2 = \sigma_3^2 = \frac{G}{(2R)^{\alpha}}$. Let $Z_1 \triangleq \sum_{m=1}^{M}\frac{2}{\sigma_1^2}|h_1^{(m)}|^2$ and $Z_2 \triangleq \sum_{k=2,m=1}^{K=3,M}\frac{2}{\sigma_k^2}|h_k^{(m)}|^2$, which are two central chi-square random variables with $2M$ and $4M$ degrees of freedom, respectively. Then, the expected value and the variance of the SNR shown in (24) can be obtained as follows:

$$E[SNR] = \frac{\sigma_1^2 P}{2N}2M + \frac{\sigma_2^2 P}{2N}4M = \frac{P}{N}\left(\sigma_1^2 M + 2\sigma_2^2 M\right); \tag{25}$$

$$Var[SNR] = 4\left(\frac{\sigma_1^2 P}{2N}\right)^2 M + 8\left(\frac{\sigma_2^2 P}{2N}\right)^2 M. \tag{26}$$

According to (23), we have the following equations to solve for s:

$$\frac{\sigma_1^4}{2}M + \sigma_2^4 M = \frac{1}{s}\left(\sigma_1^2 M + 2\sigma_2^2 M\right)^2, \tag{27}$$

which yields

$$s = 2M\frac{\left(\sigma_1^2 + 2\sigma_2^2\right)^2}{\sigma_1^4 + 2\sigma_2^4} = 2M\frac{\left(7^{-\alpha/2} + 2^{1-\alpha}\right)^2}{7^{-\alpha} + 2^{1-2\alpha}}, \tag{28}$$

and thus

$$\delta = \frac{E[SNR]}{s} = \frac{P\left(\sigma_1^4 + 2\sigma_2^4\right)}{2N\left(\sigma^2 + 2\sigma_2^2\right)} = \frac{PG\left(7^{-\alpha} + 2^{1-2\alpha}\right)}{2NR^{\alpha}\left(7^{-\frac{\alpha}{2}} + 2^{1-\alpha}\right)}. \tag{29}$$

Following [29], the SNR is approximated by $Z = \delta\Psi$, where Ψ is distributed as a chi-square random variable with s degrees of freedom, so the outage probability can be approximated as

$$\begin{aligned} P_{\text{out}}(\sharp7) &= Pr[SNR \leqslant \gamma_0] \approx Pr[Z \leqslant \gamma_0] = Pr\left[\Psi \leqslant \frac{\gamma_0}{\delta}\right] \\ &= \frac{\gamma\left(\frac{s}{2}, \frac{\gamma_0 NR^{\alpha}\left(7^{-\alpha/2}+2^{1-\alpha}\right)}{PG(7^{-\alpha}+2^{1-2\alpha})}\right)}{\Gamma(s/2)}, \end{aligned} \tag{30}$$

where $\Gamma(x) = \int_0^{\infty} t^{x-1}e^{-t}dt$ is the Gamma function.

TABLE III
OUTAGE PROBABILITIES OF ASYMMETRIC BS ARRANGEMENTS

Modes	s	P_{out}
$\sharp 2$	$2M\frac{\left[\left(\frac{3}{2}\sqrt{3}\right)^{-\alpha}+2\left(\frac{\sqrt{21}}{2}\right)^{-\alpha}+2\left(\frac{3}{2}\right)^{-\alpha}\right]^2}{\left(\frac{27}{4}\right)^{-\alpha}+2\left(\frac{21}{4}\right)^{-\alpha}+2\left(\frac{9}{4}\right)^{-\alpha}}$	$\frac{\gamma\left(\frac{s}{2},\frac{N\gamma_0 R^\alpha\left[\left(\frac{3}{2}\sqrt{3}\right)^{-\alpha}+2\left(\frac{\sqrt{21}}{2}\right)^{-\alpha}+2\left(\frac{3}{2}\right)^{-\alpha}\right]}{PG\left[\left(\frac{27}{4}\right)^{-\alpha}+2\left(\frac{21}{4}\right)^{-\alpha}+2\left(\frac{9}{4}\right)^{-\alpha}\right]}\right)}{\Gamma\left(\frac{s}{2}\right)}$
$\sharp 3(\alpha=3)$	$4M\frac{\left[\left(\frac{3}{2}\right)^{-\alpha}+\left(\frac{\sqrt{21}}{2}\right)^{-\alpha}\right]^2}{\left(\frac{9}{4}\right)^{-\alpha}+\left(\frac{21}{4}\right)^{-\alpha}}=6.0807M$	$\frac{\gamma\left(\frac{s}{2},\frac{N\gamma_0 R^\alpha\left[\left(\frac{3}{2}\right)^{-\alpha}+\left(\frac{\sqrt{21}}{2}\right)^{-\alpha}\right]}{PG\left[\left(\frac{9}{4}\right)^{-\alpha}+\left(\frac{21}{4}\right)^{-\alpha}\right]}\right)}{\Gamma\left(\frac{s}{2}\right)}=\frac{\gamma\left(3.0404M,4.0065\frac{N\gamma_0 R^3}{PG}\right)}{\Gamma(3.0404M)}$
$\sharp 4$	$4M\frac{\left[2^{-\alpha}+\left(\sqrt{7}\right)^{-\alpha}\right]^2}{\left(4^{-\alpha}+7^{-\alpha}\right)}$	$\frac{\gamma\left(\frac{s}{2},\frac{N\gamma_0 R^\alpha\left[2^{-\alpha}+\left(\sqrt{7}\right)^{-\alpha}\right]}{PG\left(4^{-\alpha}+7^{-\alpha}\right)}\right)}{\Gamma\left(\frac{s}{2}\right)}$
$\sharp 5(\alpha=3)$	$7.4343M$	$\frac{\gamma\left(3.7171M,5.0410\frac{N\gamma_0 R^3}{PG}\right)}{\Gamma(3.7171M)}$
$\sharp 5(\alpha=4)$	$7.3808M$	$\frac{\gamma\left(3.6904M,8.6892\frac{N\gamma_0 R^4}{PG}\right)}{\Gamma(3.6904M)}$
$\sharp 7$	$2M\frac{\left(\sigma_1^2+2\sigma_2^2\right)^2}{\sigma_1^4+2\sigma_2^4}=2M\frac{\left(7^{-\alpha/2}+2^{1-\alpha}\right)^2}{7^{-\alpha}+2^{1-2\alpha}}$	$\frac{\gamma\left(\frac{s}{2},\frac{\gamma_0 N R^\alpha\left(7^{-\alpha/2}+2^{1-\alpha}\right)}{PG\left(7^{-\alpha}+2^{1-2\alpha}\right)}\right)}{\Gamma(s/2)}$
$\sharp 8$	$2M\frac{\left[\left(\frac{3\sqrt{3}}{2}\right)^{-\alpha}+2\left(\frac{\sqrt{21}}{2}\right)^{-\alpha}\right]^2}{\left(\frac{27}{4}\right)^{-\alpha}+2\left(\frac{21}{4}\right)^{-\alpha}}$	$\frac{\gamma\left(\frac{s}{2},\frac{N\gamma_0 R^\alpha\left[\left(\frac{3\sqrt{3}}{2}\right)^{-\alpha}+2\left(\frac{\sqrt{21}}{2}\right)^{-\alpha}\right]}{PG\left[\left(\frac{27}{4}\right)^{-\alpha}+2\left(\frac{21}{4}\right)^{-\alpha}\right]}\right)}{\Gamma\left(\frac{s}{2}\right)}$
$\sharp 12$	$2M$	$\frac{\gamma\left(M,\frac{N\gamma_0 R^\alpha\left(\sqrt{7}\right)^\alpha}{PG}\right)}{(M-1)!}$

Similarly, we can obtain the worst-case probabilities of other cooperating modes with asymmetric BS arrangements and summarize in Table III.

C. Overall Channel Outage Probability

The overall channel outage probability for the UE in the moon cell can be obtained by combining the individual channel outage probability of every cooperating mode according to their relative frequencies. Specifically, the overall channel outage probability of pattern $w \in \{I, II, III, IV\}$ is obtained as follows,

$$P_{\texttt{overall}}(w) = \sum_{i=1}^{12} f_i(w,E)\, P_{\texttt{out}}(\sharp i) \tag{31}$$

where $f_i(w,E) \triangleq \frac{N_i(w,E)}{\sum_{i=1}^{12} N_i(w,E)}$ is the relative frequency of the $i-$th cooperating mode under pattern w among all the 12 cooperating modes shown in Fig. 3, when the offered load of each cell is E; $P_{\texttt{out}}(\sharp i)$ is the worst-case channel outage probability of cooperating mode $\sharp i$.

The relative frequency of each cooperating mode can be obtained by conducting a computer simulation of the system dynamics. For each switch-off pattern based on the system model introduced in Section II, we count the frequency of each cooperating mode over a large number of time quanta. In this simulation, each cell (either sun cell or moon cell) supplies an i.i.d. offered load of E to the infrastructure. The offered load is then aggregated at each active BS which has a limited capacity of C active concurrent UEs, according to the chosen switch-off pattern. The histograms of the relative frequencies of the cooperating modes under each pattern is shown with both low and high traffic loads in Section VI.

V. ENERGY SAVING ANALYSIS

In this section, we quantify the energy saving achieved by the proposed scheme. When a BS is switched off, only a negligible amount of energy is consumed[5]. When a BS is on, the total power consumption $P_{\texttt{total}}$ of an active BS can be divided into two main parts [32], [33]:

- The idle power consumption, represented by $P_{\texttt{idle}}$, which does not depend on the network traffic load. This power is consumed as long as a BS is on, even if there is little traffic load.
- The transmit power consumption, represented by $P_{\texttt{RF}}$, which depends on the network traffic load. This part mainly includes the consumption of the radio frequency (RF) output components. Specifically, we model $P_{\texttt{RF}}$ as $P_{\texttt{RF}} = E\frac{P_{\texttt{RF,Peak}}}{E_{\texttt{Peak}}}$, where $E_{\texttt{Peak}}$ denotes the offered load during peak hours, and $P_{\texttt{RF,Peak}}$ represents a BS's total transmit power consumption during peak hours under conventional operation (with all BSs remaining active).

We also assume that the additional baseband signal processing power consumed due to cooperation among active BSs is negligible compared to the aforementioned two main parts.

Define $\eta \triangleq \frac{P_{\texttt{RF,Peak}}}{P_{\texttt{idle}}}$, then the energy consumption per BS under the conventional operation can be calculated as follows:

$$D_{\texttt{conv}} = P_{\texttt{idle}} + E\frac{P_{\texttt{RF,Peak}}}{E_{\texttt{Peak}}} = P_{\texttt{idle}}\left(1+\eta\frac{E}{E_{\texttt{Peak}}}\right), \tag{32}$$

where $P_{\texttt{RF,Peak}}$ is assumed to be just enough to guarantee the channel outage probability of the UE at the worst case location under conventional operation during peak hours.

[5]This very small amount of energy is consumed by some mechanism of a turned-off BS to turn it back on. For simplicity, we approximate such an amount close to zero, considering that such mechanism can be implemented through a network interface to the backhaul network (dedicated wired network) which consumes a negligible amount of power.

TABLE IV
SYSTEM PARAMETERS

Switch-off Patterns	I, II, III, IV
Offered Load E	[0:2:40] (Erlang)
BS Service Capacity C	50
Cell Radius R	Normalized to 1
Number of antennas at BS M	4
Number of antennas at the UE	1
$\phi = \frac{P}{\gamma_0 N R^\alpha / G}$	[-10:5:25] dB
$\eta = \frac{P_{\mathtt{RF,Peak}}}{P_{\mathtt{idle}}}$	10%
$E_{\mathtt{Peak}}$	40 (Erlang)
Path-loss Exponent α	4
QoS Threshold: Call-blocking Probability	$\leqslant 2\%$
QoS Threshold: Channel Outage Probability	$\leqslant 10^{-3}$

During energy-efficient operations, the UEs of the sun cell are served by the single BS inside the sun cell in the same way of conventional operation. Meanwhile, depending on which pattern to use, a portion β of BSs are switched off, resulting in $\beta P_{\mathtt{idle}}$ power saving and transferring the traffic load from the moon cells to the remaining active BSs. Since the minimum requirement of channel outage probability is guaranteed for the UE at the worst-case locations through transmit power control, the calculation of the total energy consumption has to take into account the changes of $P_{\mathtt{RF}}$ for the moon cells. On the one hand, due to increased distances between the UEs of the moon cell and active BSs, the required $P_{\mathtt{RF}}$ will increase to maintain the minimum QoS requirement for the worst-case locations. On the other hand, the use of BS-cooperation helps significantly reduce such a penalty of increased $P_{\mathtt{RF}}$. We define ρ as the ratio of the total transmit power required for cooperative transmission to the transmit power required in conventional operation to maintain the same minimum channel outage probability for their corresponding worst-case locations. The *energy consumption per BS* under energy-efficient operations is defined as the ratio of the total energy consumed to serve every cell (including both moon and sun cells) to the total number of BSs (including both active and switched-off BSs), which can be written as

$$\begin{aligned} D_{\mathtt{eff}} &= (1-\beta)\left(P_{\mathtt{idle}} + P_{\mathtt{RF}}\right) + \rho\beta P_{\mathtt{RF}} \\ &= P_{\mathtt{idle}}\left[(1-\beta) + (1-\beta)\,\eta\frac{E}{E_{\mathtt{Peak}}} + \rho\beta\eta\frac{E}{E_{\mathtt{Peak}}}\right] \\ &= P_{\mathtt{idle}}\left[1-\beta+\eta\frac{E}{E_{\mathtt{Peak}}}\left(1+\beta\left(\rho-1\right)\right)\right]. \end{aligned} \tag{33}$$

VI. NUMERICAL RESULTS

In this section, we present some numerical results showing the performance and the energy saving potential of such an energy-efficient cellular network employing the proposed BS switching patterns and cooperative coverage extension scheme. In the numerical evaluations, unless otherwise stated, the system parameters are chosen as shown in Table IV.

A. Call-Blocking Probability

In this part, we present the call-blocking probabilities for the switch-off patterns and compare them with the conventional all-on pattern (i.e. all BSs are active without cooperation). As shown in Section III-B, the call-blocking probability for the sun cell always serves as an upper bound for that of the moon cell. In this paper, we guarantee the QoS of UEs by targeting at the performances of a UE situated in the worst case. In doing so, we focus the call-blocking probability of the sun cell that represents the minimum QoS level to be maintained when switching off BSs.

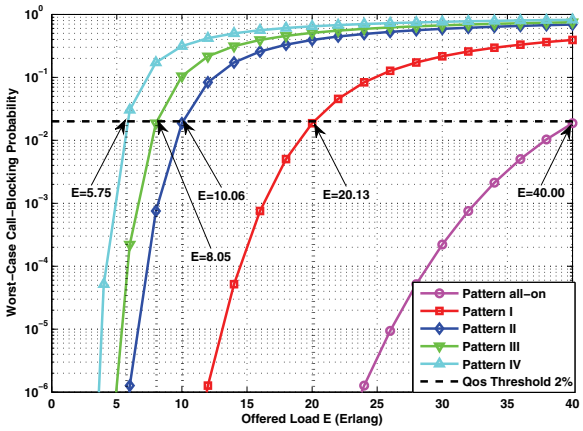

Fig. 4. The worst-case (sun cell) call-blocking probabilities versus the offered load.

Fig. 4 shows the worst-case (sun cell) call-blocking probabilities of different patterns. From Fig. 4, one can see that switching off more BSs would incur higher probability of call blocking, since each active BS is responsible for a larger aggregated traffic load. Thus, the correspondence between the pattern and the call-blocking probability characterizes a feasible set of candidate patterns so that the minimum QoS requirement on the call-blocking probability is satisfied for a given offered load. Specifically, for the numerical results shown in Fig. 4, the feasible set S is given by

$$S = \begin{cases} \{All-on, I, II, III, IV\}, & if\ E \in [0, 5.75); \\ \{All-on, I, II, III\}, & if\ E \in [5.75, 8.05); \\ \{All-on, I, II\}, & if\ E \in [8.05, 10.06); \\ \{All-on, I\}, & if\ E \in [10.06, 20.13); \\ \{All-on\}, & if\ E \in [20.13, 40.25]. \end{cases} \tag{34}$$

B. Channel Outage Probability

In this part, we show the numerical results of the channel outage probability defined and analyzed in Section IV. Fig. 5 shows the histograms of the relative frequencies of the 12 cooperating modes with various traffic loads. In Fig. 5, two observations are of interest: one is that a more conservative (i.e. turning off less BSs) pattern exhibits a better chance to have more BSs cooperatively serve the UEs than the more aggressive (i.e. turning off more BSs) pattern; the other is that given a switch-off pattern, as the traffic load grows, more BSs will be out of the cooperation because they are too busy (i.e. fully occupied) to help.

To characterize the channel outage probability, we define $\phi = \frac{P}{\gamma_0 N R^\alpha / G}$, where the denominator $\gamma_0 N R^\alpha / G$ is predefined for a given network and fixed in our simulation. The quantity ϕ represents a given SNR level normalized by the

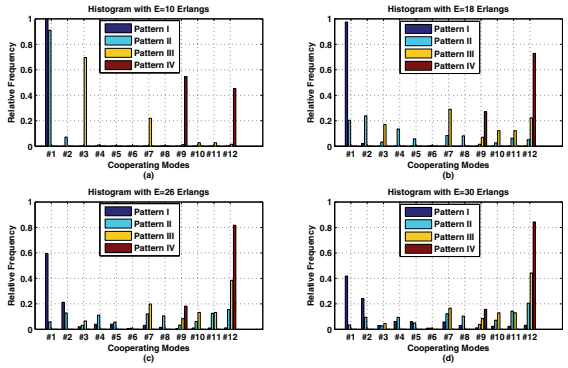

Fig. 5. The histogram of the relative frequencies of the cooperating modes under different switch-off patterns.

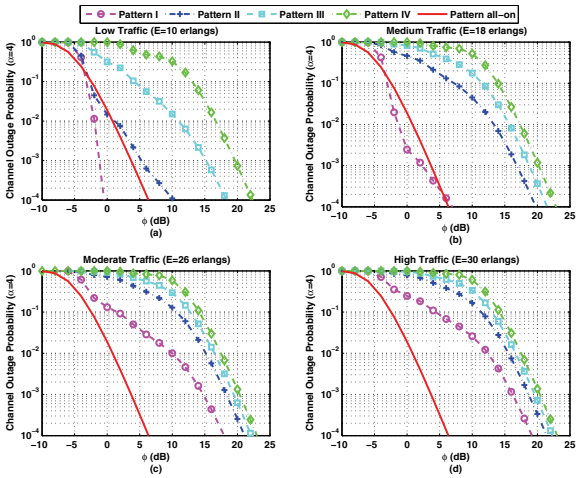

Fig. 6. The worst-case channel outage probabilities of the established link.

network- and deployment-dependent system parameters. Thus, the ratio of two ϕ values (difference in dB) is indicative of how much extra transmit power is needed to be able to move from one SNR level to the other.

Fig. 6 presents the channel outage probabilities of all the patterns with low and high traffic loads. In Fig. 6, the solid curve represents the performance of the conventional all-on pattern (or equivalently, the channel outage probability of the UE in the sun cell), which serves as a benchmark of the additional energy-efficient patterns proposed in this paper. From Fig. 6, when $E = 10$ Erlangs, to achieve a channel outage probability of 10^{-3}, Pattern I demands 4.81 dB less transmit power than the conventional pattern, resulting in $\rho(I, E = 10) = 0.3305$, thanks to the cooperation of BSs; but for the same QoS requirement, the other three switch-off patterns require more transmit power than the conventional pattern due to the increased BS-UE distances and fewer remaining active BSs, leading to $\rho(II, E = 10) = 1.1416$, $\rho(III, E = 10) = 14.23$, and $\rho(IV, E = 10) = 39.43$. As the traffic load increases, targeting at the channel outage probability of 10^{-3}, the ratios of the required transmit powers increase as shown in Table V. This is because when the traffic load is higher, the remaining active BSs will be more frequently occupied, further reducing diversity order of the BS cooperation.

TABLE V
THE RATIOS (ρ) OF THE REQUIRED TRANSMIT POWERS

	I	II	III	IV
E=10 Erlangs	$\rho = 0.3305$	$\rho = 1.142$	$\rho = 14.23$	$\rho = 39.43$
E=18 Erlangs	$\rho = 0.7300$	$\rho = 21.51$	$\rho = 33.63$	$\rho = 44.83$
E=26 Erlangs	$\rho = 13.14$	$\rho = 29.42$	$\rho = 38.51$	$\rho = 47.38$
E=30 Erlangs	$\rho = 17.91$	$\rho = 31.53$	$\rho = 39.20$	$\rho = 48.04$

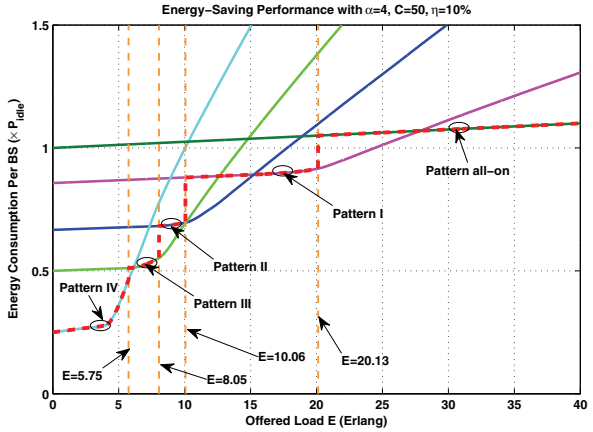

Fig. 7. The energy consumption per BS with $\alpha = 4, C = 50, \eta = 10\%$..

C. Energy-Saving Performance

The energy saving ability under different levels of offered loads, as defined in (32) and (33), is evaluated in this part. Fig. 7 shows the *energy consumption per BS* for different patterns and the corresponding energy-efficient pattern-switching strategy, with $\eta = 10\%$, the target call-blocking probability requirement of 2%, and path loss exponent $\alpha = 4$. In Fig. 7, the four vertical dashed lines indicate how much traffic load each pattern can hold with the 2% call-blocking probability requirement; the solid curves represent the energy consumption of different patterns (as marked in the figure).

From Fig. 7, one can see that no single pattern can achieve the best energy-saving performance all the time with the minimum requirement of QoS guaranteed. Therefore, a switching strategy among these patterns that jointly considers both the resulting energy consumption and the QoS requirement is desirable and characterized by the dotted curves in Fig. 7. As shown in Fig. 7, the most energy-efficient pattern is chosen according to the offered load. As the offered load varies, the pattern switching occurs whenever a more energy-efficient pattern becomes feasible (35) or the currently chosen pattern would otherwise violate the constraint of the call-blocking probability. As shown in Fig. 7, during the very low traffic period ($E < 5$), the proposed operation can save more than 50% of the energy consumed by the conventional scheme with guaranteed QoS; for about half of the period of a typical day[6], the proposed energy-efficient patterns can be applied to save energy that is currently being wasted under the conventional all-on pattern.

1) Impact of the path loss exponent: Fig. 8 shows the energy consumption results with a lower path loss exponent $\alpha = 3$, keeping the other parameters the same with Fig. 7

[6]according to the near-sinusoid daily traffic profile reported in [5]

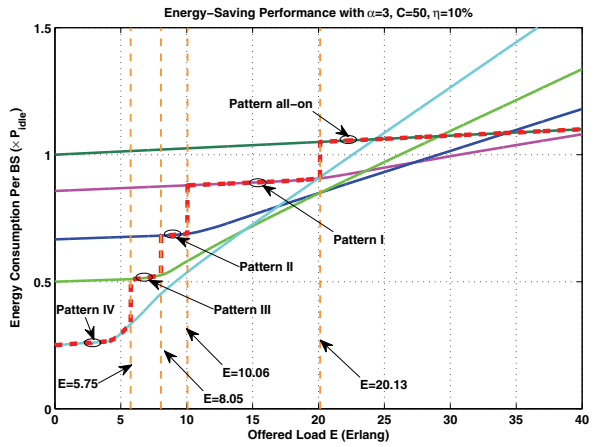

Fig. 8. The energy consumption per BS with $\alpha = 3, C = 50, \eta = 10\%$..

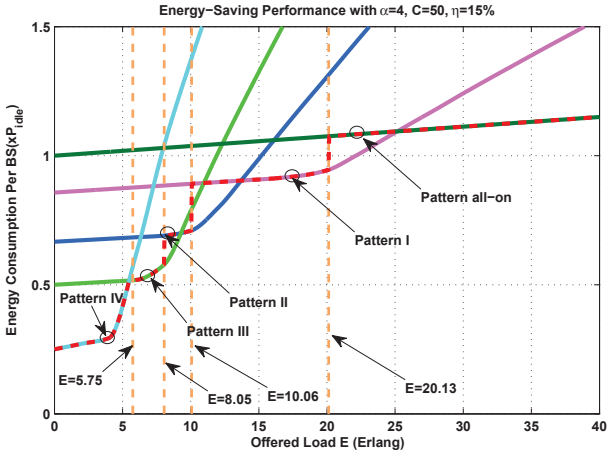

Fig. 9. The energy consumption per BS with $\alpha = 4, C = 50, \eta = 15\%$..

(i.e. $C = 50$ and $\eta = 10\%$). Comparing Fig. 7 and Fig. 8, one can see that the energy consumption with lower path loss grows much slower with the increasing offered load than the one with high path loss. This is due to the fact that with a smaller path loss, the total transmit power required to extend coverage to the moon cells is reduced, resulting a smaller ρ in (33).

2) Impact of η: Fig. 9 shows the energy consumption results with a larger $\eta = 15\%$ (with all the other parameters the same as used in Fig. 7). Comparing Fig. 9 with Fig. 7, one can see that as η increases, the more aggressive patterns[7] lose their advantages in energy saving to the more conservative patterns at smaller offer load. This is because a larger η gives a larger weighting factor to the transmit power consumption, in which case the benefit of having more cooperating BSs available in the more conservative patterns can be observed earlier at smaller offer load.

3) Impact of C: Unlike the parameters α and η which are determined by the characteristics of a given system, the service capacity C is a design parameter that can be expanded by upgrading hardware and software at the BS [20]. Therefore,

[7]Pattern IV is considered as the most aggressive pattern, while the Pattern all-on is considered as the most conservative pattern, in terms of the number of switched-off cell.

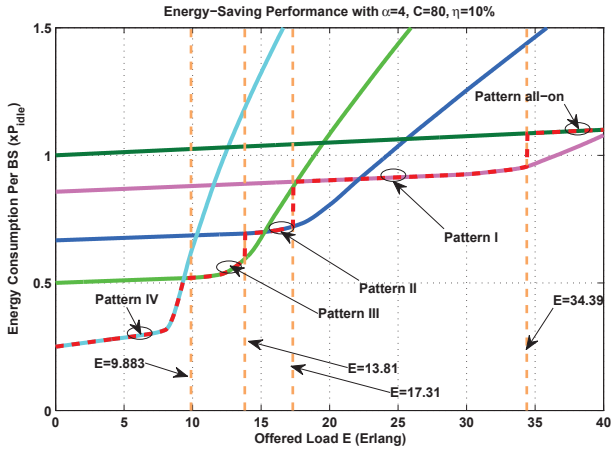

Fig. 10. The energy consumption per BS with $\alpha = 4, C = 80, \eta = 10\%$.).

it is worthwhile to study its impact to the energy saving performance. The impact of C is two-fold:

First, the service capacity C affects the call blocking probability. A larger service capacity of BS helps reduce the call blocking probability for a given offered load under any pattern, which loosens the constraint on pattern selection. For example, with a given call-blocking probability QoS threshold 2%, compared with the constraint with $C = 50$ as shown by (34), a larger $C = 80$ gives the following loosened constraint:

$$S = \begin{cases} \{All-on,\ I,\ II,\ III,\ IV\}, & if\ E \in [0, 9.883); \\ \{All-on,\ I,\ II,\ III\}, & if\ E \in [9.883, 13.81); \\ \{All-on,\ I,\ II\}, & if\ E \in [13.81, 17.31); \\ \{All-on,\ I\}, & if\ E \in [17.31, 34.39); \\ \{All-on\}, & if\ E \in [34.39, 68.70]. \end{cases} \tag{35}$$

Second, the service capacity C affects the relative frequencies of the cooperating modes. A larger service capacity of BS reduces the likelihood that an active BS is fully occupied, so that more active BSs can still participate the BS cooperation at higher offer loads, which helps reduce the required transmit power (due to cooperative beamforming).

In Fig. 10, we presented the energy consumption results with a larger service capacity $C = 80$ (with all the other parameters the same as used in Fig. 7). Comparing Fig. 10 with Fig. 7, the larger service capacity C allows the more aggressive patterns to operate at higher offered load. For example, with $C = 50$ in Fig. 7, Pattern IV has to switch to Pattern III at $E = 5.75$ Erlangs to guarantee the call-blocking probability not exceeding the 2% threshold, even though at $E = 5.75$ Erlangs Pattern IV still demands less energy than Pattern III. However, with $C = 80$ in Fig. 10, the switch between Pattern IV and Pattern III occurs at $E = 9.37$ Erlangs, which is facilitated by the fact that with $C = 80$ Pattern IV is allowed to operate up to $E = 9.883$ Erlangs without violating the 2% QoS threshold of the call-blocking probability.

VII. Conclusion and Outlook

In this paper, we propose an energy-efficient BS switching strategy in which some BSs are turned off and BS cooperation is used to effectively extend coverage with guaranteed QoS. Based on the standard hexagonal cell network model, four

switch-off patterns are introduced to progressively turn more BSs off to save energy according to the offered traffic load. We consider QoS from both the network-layer and the physical-layer perspectives, and analyze the call-blocking probability and the channel outage probability. We guarantee the QoS of the UEs under the energy-efficient patterns by focusing on the worst-case transmission/reception locations instead of just looking at the spatially averaged performance. With guaranteed QoS, the energy-saving performance of the proposed scheme is evaluated. Both the analytical and numerical results exhibit significant energy-saving potential of the proposed idea of BS switching and cooperative coverage extension.

Several implications based on this work can be useful to practical cellular networks. First, switching off some BSs during low-traffic hours according to several predetermined patterns is effective in energy-saving with feasible complexity. Although the regular hexagonal cells hardly exist in reality, the well-planned macrocell BS deployment and the consistent periodicity of traffic profiles [4], [5] afford the off-line computation of several progressive switching patterns for a certain area. Second, BS cooperation can be used to effectively extend coverage, especially when some BSs are off. Cooperation among BSs has been made available in recent standards such as LTE-advanced, referred to as Coordinated Multi-Point (CoMP), facilitating a basis for the proposed cooperative coverage extension scheme. Lastly, given the significant energy-saving potential predicted by the theoretical model, it can be worthwhile to investigate the potential signaling cost of pattern switching, UE handover, and BS Cooperation, which will be interesting future research.

REFERENCES

[1] G. Fettweis and E. Zimmermann, "ICT energy consumption-trends and challenges," in *Proc. 2008 International Symposium on Wireless Personal Multimedia Communications*.

[2] S. Fletcher, "Core 5 - Green radio: programme objectives and overview," http://www.mobilevce.com/dloads-publ/mtg284Item_1503.ppt/, 2008.

[3] M. Marsan, L. Chiaraviglio, D. Ciullo, and M. Meo, "Optimal energy savings in cellular access networks," in *Proc. 2009 IEEE International Conference on Communications Workshops*, pp. 1–5.

[4] E. Oh, B. Krishnamachari, X. Liu, and Z. Niu, "Toward dynamic energy-efficient operation of cellular network infrastructure," *IEEE Commun. Mag.*, vol. 49, no. 6, pp. 56–61, 2011.

[5] E. Oh and B. Krishnamachari, "Energy savings through dynamic base station switching in cellular wireless access networks," in *Proc. 2010 IEEE Global Telecommunications Conference*, pp. 1–5.

[6] L. Chiaraviglio, D. Ciullo, M. Meo, and M. Marsan, "Energy-aware umts access networks," in *Proc. 2008 International Symposium on Wireless Personal Multimedia Communications*.

[7] S. Zhou, J. Gong, Z. Yang, Z. Niu, and P. Yang, "Green mobile access network with dynamic base station energy saving," in *2009 ACM International Conference on Mobile Computing and Networking*.

[8] A. J. Fehske, F. Richter, and G. P. Fettweis, "Energy efficiency improvements through micro sites in cellular mobile radio networks," in *Proc. 2009 IEEE GLOBECOM Workshops*, pp. 1–5.

[9] K. Son, E. Oh, and B. Krishnamachari, "Energy-aware hierarchical cell configuration: from deployment to operation," in *Proc. 2011 IEEE Conference on Computer Communications Workshops*, pp. 289–294.

[10] M. A. Marsan and M. Meo, "Energy efficient management of two cellular access networks," *ACM SIGMETRICS Perform. Eval. Rev.*, vol. 37, no. 4, pp. 69–73, Mar. 2010.

[11] D. Cao, S. Zhou, C. Zhang, and Z. Niu, "Energy saving performance comparison of coordinated multi-point transmission and wireless relaying," in *Proc. 2010 IEEE Global Telecommunications Conference*, pp. 1–5.

[12] J. Kwak, K. Son, Y. Yi, and S. Chong, "Greening effect of spatio-temporal power sharing policies in cellular networks with energy constraints," *IEEE Trans. Wireless Commun.*, vol. 11, no. 12, pp. 4405–4415, 2012.

[13] T. Rappaport, *Wireless Communications: Principles and Practice*, 2nd ed. Prentice Hall PTR, 2001.

[14] J. S. Seybold, *Introduction to RF Propagation*. Wiley-Interscience, 2005.

[15] Z. Han and K. J. R. Liu, *Resource Allocation for Wireless Networks*. Cambridge University Press, 2008.

[16] K. J. R. Liu, A. K. Sadek, W. Su, and A. Kwasinski, *Cooperative Communications and Networking*. Cambridge University Press, 2009.

[17] A. K. Sadek, Z. Han, and K. J. R. Liu, "Distributed relay-assignment protocols for coverage expansion in cooperative wireless networks," *IEEE Trans. Mobile Comput.*, vol. 9, no. 4, pp. 505–515, 2010.

[18] T. Rappaport, *Wireless Communications: Principles and Practice*. Prentice Hall, 1996.

[19] G. Stuber, *Principles of Mobile Communication*, 2nd ed. Kluwer Academic Publishers, 2001.

[20] J. L. Z. Zhang, F. Heiser and H. Leuschner, "Advanced baseband technology in third-generation radio base stations," *Ericsson Review*, no. 1, pp. 32–41, 2003.

[21] A. J. Goldsmith, *Wireless Communications*, 1st ed. Cambridge University, 2005.

[22] M. Bublin, I. Kambourov, P. Slanina, D. Bosanska, O. Hlinka, O. Hrdlicka, and P. Svac, "Inter-cell interference management by dynamic channel allocation, scheduling and smart antennas," in *Proc. 2007 IST Mobile and Wireless Communications Summit*, pp. 1–5.

[23] H. Ochiai, P. Mitran, H. Poor, and V. Tarokh, "Collaborative beamforming for distributed wireless ad hoc sensor networks," *IEEE Trans. Signal Process.*, vol. 53, no. 11, pp. 4110–4124, 2005.

[24] D. G. Brennan, "On the maximum signal-to-noise ratio realizable from several noisy signals," in *Proc. 1955 Institute of Radio Engineers*, p. 1530.

[25] R. M. Karp, "Reducibility among combinatorial problems," in *Complexity of Computer Computations*. Plenum Press, 1972, pp. 85–103.

[26] M. R. Garey and D. S. Johnson, *Computers and Intractability; A Guide to the Theory of NP-Completeness*. W. H. Freeman & Co., 1990.

[27] D. Gross, J. F. Shortle, J. M. Thompson, and C. M. Harris, *Fundamentals of Queueing Theory*, 4th ed. John Wiley & Sons, 2008.

[28] S. Boyd and L. Vandenberghe, *Convex Optimiaztion*. Cambridge University, 2004.

[29] F. E. Satterthwaite, "Synthesis of variance," *Psychometrika*, vol. 6, no. 5, pp. 309–316, 1941.

[30] C. Alexopoulos, "Statistical analysis of simulation output: state of the art," in *Proc. 2007 Winter Simulation Conference*, pp. 150–161.

[31] R. H. Y. Louie, M. R. McKay, and I. B. Collings, "New performance results for multiuser optimum combining in the presence of rician fading," *IEEE Trans. Commun.*, vol. 57, no. 8, pp. 2348–2358, 2009.

[32] O. Arnold, F. Richter, G. Fettweis, and O. Blume, "Power consumption modeling of different base station types in heterogeneous cellular networks," in *Proc. 2010 Future Network and Mobile Summit*, pp. 1–8.

[33] O. Blume, H. Eckhardt, S. Klein, E. Kuehn, and W. M. Wajda, "Energy savings in mobile networks based on adaptation to traffic statistics," *Bell Lab. Tech. J.*, vol. 15, no. 2, pp. 77–94, Sep. 2010.

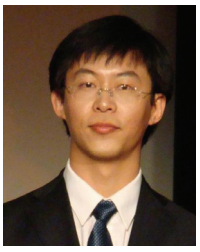

Feng Han (S'08) received the B.S. and M.S. degrees in Electronic Engineering from Tsinghua University, Beijing, China, in 2007 and 2009, respectively. He is currently a Ph. D. Candidate in Electrical Engineering, at the University of Maryland, College Park. His current research interests include wireless communications and networking, game theory, signal processing and communication theory.

He is a recipient of the first prize in the 19th Chinese Mathematical Olympiad, the Best Thesis Award of Tsinghua University, the honor of Excellent Graduate of Tsinghua University, the A. James Clark School of Engineering Distinguished Graduate Fellowship in 2009 and the Future Faculty Fellowship in 2012, both from the University of Maryland, College Park. His work on time reversal technique was recognized by the university-level Invention of the Year Award at University of Maryland in 2013, and his work on MIMO system received a Best Paper Award for at IEEE WCNC'08, Las Vegas, NV, in 2008.

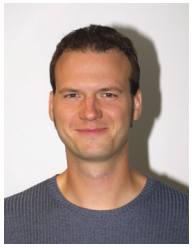

Zoltan Safar (M'04) received the University Diploma in electrical engineering from the Technical University of Budapest, Budapest, Hungary, in 1996, and the M.S. and Ph.D. degrees in electrical and computer engineering from the University of Maryland, College Park, MD, USA, in 2001 and 2003, respectively.

After graduation, he was an assistant professor in the Department of Innovation, IT University of Copenhagen, Denmark until March 2005. Then, he joined Nokia in Copenhagen, where he worked as a senior engineer on 3GPP Long Term Evolution (LTE) reciver algorithm design. From September 2007, he was a senior engineer with Samsung Electro-Mechanics in Atlanta, GA, USA, developing physical-layer signal processing algorithms for next-generation wireless communication systems. In February 2010, he became a senior software engineer at Bloomberg L.P., NY, USA, and he designed and implemented software systems for monitoring, configuration and maintenance of the company's private communication network. Since October 2010, he has been with the Department of Electrical and Computer Engineering at the University of Maryland, MD, USA, where he is the Director of the MS in Telecommunications program.

His research interests include wireless communications and statistical signal processing, with particular focus on multi-antenna wireless communication systems, OFDM receiver algorithm design, and wireless indoor surveillance.

Dr. Safar received the Outstanding Systems Engineering Graduate Student Award from the Institute for Systems Research, University of Maryland in 2003, and the Invention of the Year Award (together with W. Su and K. J. R. Liu) from the University of Maryland in 2004.

K. J. Ray Liu (F'03) was named a Distinguished Scholar-Teacher of University of Maryland, College Park, in 2007, where he is Christine Kim Eminent Professor of Information Technology. He leads the Maryland Signals and Information Group conducting research encompassing broad areas of signal processing and communications with recent focus on cooperative and cognitive communications, social learning and network science, information forensics and security, and green information and communications technology.

Dr. Liu is the recipient of numerous honors and awards including IEEE Signal Processing Society Technical Achievement Award and Distinguished Lecturer. He also received various teaching and research recognitions from University of Maryland including university-level Invention of the Year Award; and Poole and Kent Senior Faculty Teaching Award, Outstanding Faculty Research Award, and Outstanding Faculty Service Award, all from A. James Clark School of Engineering. An ISI Highly Cited Author, Dr. Liu is a Fellow of IEEE and AAAS.

Dr. Liu is President of IEEE Signal Processing Society where he has served as Vice President - Publications and Board of Governor. He was the Editor-in-Chief of *IEEE Signal Processing Magazine* and the founding Editor-in-Chief of *EURASIP Journal on Advances in Signal Processing*.